Available online at www.sciencedirect.com
ScienceDirect
Journal of Power Sources 166 (2007) 411–418
JOURNAL OF POWER SOURCES
www.elsevier.com/locate/jpowsour

The efficient and economic design of PEM fuel cell systems by multi-objective optimization

Woonki Na [1], Bei Gou [*,2]

Energy System Research Center at the University of Texas at Arlington, Arlington, TX 76019, United States

Received 14 November 2006; received in revised form 1 January 2007; accepted 2 January 2007
Available online 17 January 2007

Abstract

Since the efficiency of fuel cells is the ratio of the electrical power output and the fuel input, it is a function of power density, system pressure, and stoichiometric ratios of hydrogen and oxygen. Typically, the fuel cell efficiency decreases as its power output increases. In order for the fuel cell system to obtain highly efficient operation with the same power generation, more cells and other auxiliaries such as a high-capacity compressor system, etc. are required. In other words, fuel cell efficiency is closely related to fuel cell economics. Therefore, an optimum efficiency should exist and should result in the definition of a cost-effective fuel cell system. Using a multi-objective optimization technique, the sequential quadratic programming (SQP) method, the efficiency and cost of a fuel cell system have been optimized under various operating conditions. This paper has obtained some analytical results that provide a useful suggestion for the design of a cost-effective fuel cell system with high operation efficiency. Published by Elsevier B.V.

Keywords: Polymer electrolyte membrane fuel cells; Multi-objective optimization

1. Introduction

A fuel cell is an electro-chemical energy device that converts the chemical energy of fuel directly into electricity and heat, with water as a by-product of the reaction. As a renewable energy source, fuel cells are widely considered one of the most promising energy sources because of their high energy efficiency, extremely low emission of oxides of nitrogen and sulfur, and very low noise, as well as the cleanness of their energy production. Based on the types of electrolytes used, they are categorized into polymer electrolyte membrane fuel cells (PEMFCs), solid oxide fuel cells (SOFCs), phosphoric acid fuel cells (PAFCs), molten carbonate fuel cells (MCFCs), and direct methanol fuel cells (DMFCs) [1]. The PEMFC has particularly attracted more attention for transportation applications because of its higher power density, faster start-up, and quick response to load changes than other fuel cells [2,3]. In addition, the PEMFC operates within a low temperature range (60–80 °C) and has a relatively simple design [1]. Due to these multiple advantages, the PEMFC has become the best candidate for an alternative power source in transportation and stationary power systems. To commercialize the PEMFC, cost and efficiency need to be taken into account. Thus, achieving an optimal PEMFC system design has become a major topic in recent years. For stationary and transportation applications, fuel cells are required to achieve and efficiency equal to or higher than 40% [3]. However, because the efficiency decreases as the power output increases [3], as more cells request power, more expenses need to be integrated to achieve a high efficiency for the maximum power output. To date, although many techniques of optimization of fuel cell systems have been developed, but many of them [5,6] are restricted to only one optimization objective, such as performance or cost. However, because these different optimization objectives are coupled or affect one another, considering only one is not realistic or practical. Recently, a few studies of multiple objectives concerning the cost and performance of fuel cell systems have been reported in literature [4]. Xue and Dong [4] searched for the optimal design of a Ballard fuel cell system with consideration of the system's performance and cost. In their work, two system parameters, the active stack intersection area and the air stoichiometric ratio, were selected as the design variables in the joint optimization. Frangopoulos and Nakos [7] studied

* Corresponding author. Tel.: +1 817 272 5049; fax: +1 817 272 5042.
E-mail address: bgou@uta.edu (B. Gou).
[1] Student Member, IEEE.
[2] Member, IEEE.

0378-7753/$ – see front matter. Published by Elsevier B.V.
doi:10.1016/j.jpowsour.2007.01.022

Table 1
Cell voltage parameters

Parameter	Value and definition
N	Cell number
E_o	Open-cell voltage (V)
R	Universal gas constant (J g^{-1} mol^{-1} K^{-1})
T	Temperature of the fuel cell (K)
F	Faraday constant (C mol^{-1})
σ	Charge transfer coefficient
i	Output current density (A cm^{-2})
i_o	Exchange current density (A cm^{-2})
i_n	Internal current density (A cm^{-2})
m and n	Constants in the mass transfer voltage
r	Area-specific resistance (kΩ cm^{-2})

the optimal design of the 5-kW PEM fuel cell in which the fuel cell power density and the present worth of the life-cycle cost of the system were used as the objectives of optimization. In our study, a multi-objective optimization technique is applied to optimize two objectives, the efficiency and the cost of the fuel cell system under different operating conditions. In contrast to previous research [4,7], our paper defines the system pressure, the hydrogen and air stoichiometric ratios, and the cell voltage and current density as design variables, which means that it provides a broader insight into the optimal fuel cell design. Under the variations in these variables, the structure of a more cost-effective fuel cell system with a high efficiency level will be determined (Table 1).

This paper is organized as follows. Section 2 gives a concept of PEMFC and its efficiency. Section 3 addresses the design of the PEMFC cost model for the optimization. In Section 4, the multi-objective optimization for the PEMFC is presented. Section 5 provides the results and a discussion with regard to the optimization. Section 6 concludes the paper.

2. PEM fuel cell and efficiency

A PEMFC consists of the polymer electrolyte membrane sandwiched between two electrodes (anode and cathode). In the electrolyte, only ions can exit, while electrons are not allowed to go through. Thus, the flow of electrons needs a path like an external circuit from the anode to the cathode to produce electricity because of a potential difference between the anode and cathode. The overall electro-chemical reactions for a PEM fuel cell fed with a hydrogen-containing anode gas and an oxygen-containing cathode gas, are given as follows:

$$\text{Anode}: \quad 2H_2 \leftrightarrow 4H^+ + 4e^-$$

$$\text{Cathode}: \quad O_2 + 4H^+ + 4e^- \leftrightarrow 2H_2O$$

$$\text{Overall}: \quad 2H_2 + O_2 \leftrightarrow 2H_2O + \text{electricity} + \text{heat}$$

In practice, a 5-kW fuel cell stack, such as a Ballard MK5-E PEMFC stack, uses a pressurized hydrogen tank at 10 atm and oxygen taken from atmospheric air [10].

At the anode side, a fuel processor, called a reformer, which generates hydrogen through reforming methane or other fuels like natural gas, can be used instead of the pressurized hydrogen tank. A pressure regulator and purging of the hydrogen component are also needed. At the cathode side, there is an air supply system that contains a compressor, air filter, and air flow controller to maintain the oxygen partial pressure [1,12,14]. At both sides, a humidifier is required to prevent dehydration of the fuel cell membrane [1,12,14]. In addition, a heat exchanger, water tank, water separator, and pump may also be needed for water and heat management in the FC systems [1,12,14].

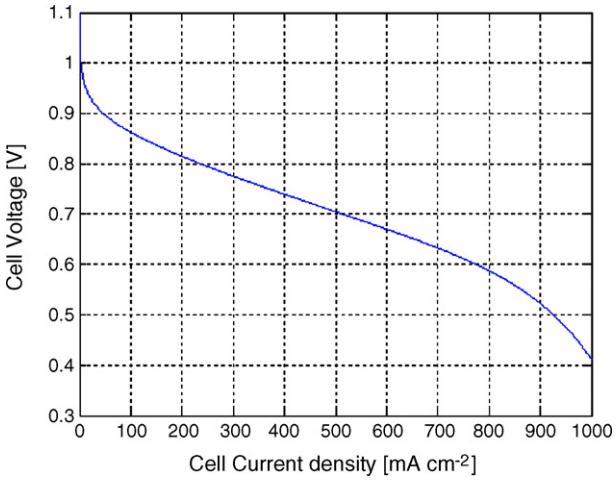

Fig. 1. Polarization curve (Ballard Mark V PEMFC at 70 °C) [1].

To produce a higher voltage, multiple cells must be connected in series. Typically, a single cell produces a voltage between 0 and 1 V based on the polarization I–V curve, which expresses the relationship between stack voltage and load current [1]. As shown in Fig. 1, this voltage is nonlinear and mainly depends on current density, cell temperature, reactant partial pressure, and membrane humidity [1] (Fig. 2).

The output stack voltage V_{st} [1] is defined as a function of the stack current, reactant partial pressures, fuel cell temperature, and a membrane humidity, as follows:

$$V_{st} = E - V_{activation} - V_{ohmic} - V_{concentration}. \quad (1)$$

In above equation,

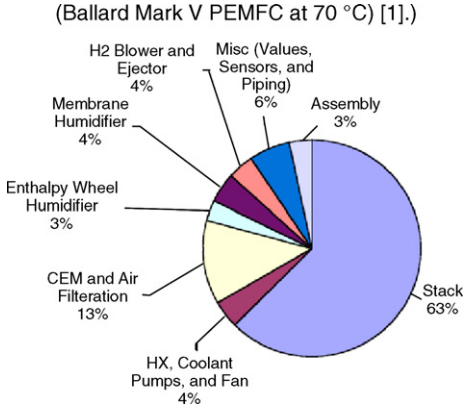

Fig. 2. Breakdown in stack and BOP component cost contribution for an 80-kW direct hydrogen fuel cell system [17].

Table 2
Ballard Mark V PEMFC coefficients [14]

Coefficients	Values (T in °C)
E_{oc} (V)	1.05
C (V)	4.01×10^{-2} to $1.4 \times 10^{-4}T$
r ($k\Omega\,cm^{-2}$)	4.77×10^{-4} to $3.32 \times 10^{-6}T$
m (V); $T \geq 39$ °C	1.1×10^{-4} to $1.2 \times 10^{-6}T$
m (V); $T \leq 39$ °C	3.3×10^{-3} to $8.2 \times 10^{-5}T$
n ($cm^2\,mA^{-1}$)	8.0×10^{-3}

$E = N[E_o + (RT/2F)\ln((P_{H_2}\sqrt{P_{O_2}})/P_{H_2O_c})]$ is the thermodynamic potential of the cell or reversible voltage based on the Nernst equation [1]. $V_{activation}$ is the voltage loss due to the rate of reactions on the surface of the electrodes. V_{ohmic} is the ohmic voltage drop from the resistances of proton flow in the electrolyte. $V_{concentration}$ is the voltage loss from the reduction in concentration gases or the transport of a mass of oxygen and hydrogen. Their equations are given as follows:

$$V_{activation} = N\frac{RT}{2\alpha F}\ln\left(\frac{i+i_n}{i_o}\right) = NCn\left(\frac{i+i_n}{i_o}\right) \quad \left(C = \frac{RT}{2\sigma F}\right) \tag{2}$$

$$V_{ohm} = Nir \tag{3}$$

$$V_{concentration} = Nm\,\exp(ni). \tag{4}$$

In Eq. (1), P_{H_2}, P_{O_2}, and $P_{H_2O_c}$ are the partial pressures of hydrogen, oxygen, and water. Subscript 'c' means that the water partial pressure is vented from the cathode side.

The concentration voltage loss is simplified by neglecting i_n, which is a very small value compared with i, and combining i_o of the Tafel equation, with $NA\ln(i)$ [1]. In practice, the Ballard mark V fuel cell voltage per cell is described in Eq. (5), which has the specific coefficients given by Table 2.

$$V_c = E_{oc} - ri - C\ln(i) - m\,\exp(ni). \tag{5}$$

The detail explanation of each voltage loss can be found in Ref. [1]. In the Nernst equation, the ideal standard potential E_o for a PEMFC is 1.229 V with a liquid water product, or 1.18 V with a gaseous water product [8]. Under the assumption that pressure on both the cathode and the anode is approximately the same, the Nernst equation is transferred into a function of the system pressure P_{sys} [1,9] given as follows.

$$E = E_o + \frac{RT}{2F}\ln\left(\frac{\alpha\beta^{1/2}}{\delta}\right) + \frac{RT}{4F}\ln(P_{sys}) \tag{6}$$

where α, β, and δ are constants depending on the molar masses and concentrations of H_2, O_2, and H_2O. Each partial pressure can be expressed by these constants and the system pressures.

$$\begin{aligned} P_{H_2} &= \alpha P_{sys} \\ P_{O_2} &= \beta P_{sys} \\ P_{H_2O} &= \delta P_{sys} \end{aligned} \quad . \tag{7}$$

Assuming that α, β, and δ are constants, Eq. (9) shows that the EMF of a fuel cell is increased due to the system pressure P_{sys}. Hence, P_{sys} can be used as one of the optimization design variables. For the multi-objective optimization, the specification of the fuel cell stacks has to be identified in advance, and then each optimization model can be derived.

First, the fuel cell efficiency optimization model is derived based on Ref. [10], and the output power of the fuel cell system is described by the following equations.

$$P_{fcs} = P_{stack} - P_{prs}. \tag{8}$$

$$P_{stack} = NiV_cA = 50\,kW. \tag{9}$$

$$P_{prs} = P_{comp} + P_{oth}. \tag{10}$$

$$P_{comp} = c_p\frac{T_e}{\eta_m\eta_{mt}}\left(\left(\frac{P_{sys}}{P_{in}}\right)^{0.286} - 1\right)\dot{m}. \tag{11}$$

$$\dot{m} = 3.57 \times 10^{-7} \times \lambda_{air} \times i \times A \times N\,kg\,s^{-1}, \tag{12}$$

where P_{fcs} is the net power of the fuel cell system and P_{stack} is the stack output power. The parasitic power consumed by the compressor is P_{comp} and the others is P_{oth}. Even though P_{oth} was assumed to be a constant of 2 kW in Ref. [10] based on 62.5 kW-rated stack power, here it is 5% of the nominal power out, 50 kW, due to the inclusion of unexpected power consumption,. Thus, P_{oth} is assumed to be 2.5 kW. The flow rate of air $\dot{m}$ is related to the air stoichimetry, the cell current density, and the active cell area. Before proceeding to build the efficiency optimization model, let us consider how to determine the optimal cell number and cell area. Once optimal current density and cell voltage have been decided, the total active cell area ($N \times A$) can be calculated by using optimal power density, the product of V_c and I, i.e., we can decide on a number of cells, as long as a single active cell area is given. The system pressure of the fuel cell is always higher than the atmospheric pressure in a certain range because the compressor cannot provide a pressure under the atmospheric pressure. According to Ref. [11], P_{sys} must be 0.02 MPa higher than the inlet air pressure P_{in}, so it is included as one of constraints in the optimization. Thus, if using the lower heating value (LHV), the fuel cell efficiency optimization model is obtained to achieve the maximum efficiency of the fuel cell in Eq. (13).

$$\max \eta_{fc}(P_{sys}, \lambda_{H_2}, \lambda_{air}, V_c, i) = \frac{V_c u_f (P_{stack} - P_{prs})}{1.25 P_{stack}}$$

s.t.

$$\begin{aligned} &P_{sys} \geq 0.12\,MPa \\ &\lambda_{H_2} \geq 1 \\ &\lambda_{air} \geq 1 \\ &V_c \geq 0\,V \\ &i \geq 0\,mA\,cm^{-2} \end{aligned} \quad . \tag{13}$$

where u_f is the fuel utilization rate, which is the reverse of the hydrogen stoichiometric ratio [12]. The air stoichiometric ratio must be over the minimum limit in order to prevent the depletion

of oxygen at this minimum limit. The hydrogen stoichiometric ratio also is greater than 1 unless it runs in the hydrogen dead-ended mode [12]. Normally, a higher air and hydrogen stoichiometric ratio is preferred in low power ranges. The ranges of cell voltage and current density will be based on the *V–I* polarization curve. Since the cell voltage is a function of the cell current density, as seen in Eq. (5), we can select four optimization parameters: system pressure, air and hydrogen stoichiometric ratios, and cell current density. By using four optimization parameters, the optimization model has been built. In the following section, the fuel cell cost optimization model will be presented.

3. PEM fuel cell cost model

For this analysis, we are particularly interested in the small and middle-sized fuel cell systems. We use a 50-kW PEM fuel cell system for transportation as the example of our study. For the fuel cell cost model, the cost of fuel cell stack and balance of plant (BOP) components for water, thermal, and fuel management were assessed. Due to lack of the latest data about hydrogen storage, power electronics, electric drive motors, hybrid batteries for PEM fuel cell systems, the fuel storage and fuel generation components were excluded in this study. The target cost is the cost of the fuel cell stack and the BOP system, given as follows:

$$C = C_{st} + C_{BOP}, \tag{14}$$

where C_{st} is the cost of the fuel cell stack and C_{BOP} is the cost of the balance of plants. For C_{st}, currently two types of fuel cell stack cost models are available in Refs. [13,16]. One is represented by the following equation [13].

$$C_{st1} = M\left[\left(\frac{A-105.4}{10} + \frac{17.56 L_p C_p}{380}\right)\frac{P_G(1+d)^N}{P_d} + B\right] \tag{15}$$

where M is a fixed-cost markup (1.1 default); A and B the cost parameter that depends on production; volume (see Table 3); L_p the fuel cell platinum loading for both electrodes (mg cm^{-2}); C_p the cost of platinum (US$ troy^{-1} oz^{-1}); P_G the fuel cell gross dc peak power (kW); P_d the fuel cell power density (W cm^{-2}); d the annual fuel cell degradation (% year^{-1}); and N is the planned fuel cell lifetime (years).

Table 3
Specification of the fuel cell system based on Ref. [1]

Items	Specification
Nominal power output (kW)	50
Stack temperature (K)	353 (80 °C)
Inlet H_2/air humidity (%)	100
Cell open voltage, E_o (V)	1.05
Entry air temperature, T_e (K)	288 (15 °C)
Specific heat constant, c_p (J K^{-1} kg^{-1})	1004
Compressor efficiency, η_c	0.75
Compressor connecting efficiency, η_m	0.85
Inlet pressure, P_{in} (Pa)	10^5

Table 4
Fuel cell stack cost parameters

Production volume	Cost parameter, A (US$ m^{-2})	Cost parameter, B (US$)
100	811.77	1311.30
1,000	722.54	363.33
10,000	454.45	428.51
30,000	329.24	405.79
60,000	312.26	160.98

The parameter A is the power-dependent term with regard to US$ m^{-2} of the membrane area, and the parameter B is the fixed cost for the fuel cell stack.

In Ref. [14], the annual fuel cell degradation is assumed to be a 6% year^{-1} drop, and the planned fuel cell lifetime is assumed to be 87,600 h, 10 years. The platinum loading, L_p, is defined as 0.4 mg cm^{-2}, and the cost of platinum, C_p, is US$ 1160 troy^{-1} oz^{-1}. Although this C_{st1} (US$) model is used in Ref. [7], it is not logically understandable because many constants and parameters (M, A, and B) are involved in Eq. (15) without justification. Thus, a more reasonable stack cost model C_{st2} is chosen from Refs. [17,18] in our study. The C_{st2} (US$ kW^{-1}) is described as follows:

$$C_{st2} = \frac{C_m + C_e + C_b + C_{pt} + C_o}{P} + C_a \tag{16}$$

$$C_{pt} = C_{wpt} \times Y_{pt} \tag{17}$$

$$P = 10 \times V_c \times i. \tag{18}$$

where C_{st2} is the fuel cell stack cost per kW (US$ kW^{-1}); C_m the membrane cost (US$ m^{-2}); C_e the electrode cost (US$ m^{-2}); C_b the bi-polar plates cost (US$ m^{-2}); C_{pt} the cost of platinum catalyst loading (US$ m^{-2}); C_{wpt} the weight of platinum catalyst loading (g m^{-2}), Y_{pt} the unit cost of platinum (US$ g^{-1}); C_o is the cost of peripheral materials (US$ m^{-2}) that include end plates, plastic frame, and thrust volts; C_a the assembly cost (US$ kW^{-1}); V_c the cell voltage; and i is the cell current density (A cm^{-2}) (Table 4).

In Refs. [17,18] the cost of each component of a 50-kW PEM fuel cell stack was estimated based on an automatic production line with an annual production capacity of 18,000 vehicles.

Table 5 shows the specific costs of components in the PEM fuel cell stack.

As for C_{BOP}, the cost model can be found in Ref. [13] – C_{BOP}, including the air blower, humidification, radiator, stainless pump, iron pump, control electronics, actuation, piping, and

Table 5
Specific costs for components in PEM fuel cell stack [17,18]

Components	Cost
Nafion membrane (US$ m^{-2})	500
Platinum; 2–4 g m^{-2} (US$ m^{-2})	32–64
Electrode; max. 0.8 mm for single cell (US$ m^{-2})	177
Bi-polar plate; max. 4 mm (US$ m^{-2})	1650
Peripheral parts (US$ m^{-2})	15.6
Assembly (US$ kW^{-1})	7.7

valves – which is approximated by a quadratic equation in the fuel cell output power and varies with the production volume, as shown the following equations [13].

For 100 production units:

$$C_a = 3343.5 + 39.942P_G - 0.0454P_G^2. \quad (17a)$$

For 10,000 production units:

$$C_a = 2980.2 + 35.654P_G - 0.0422P_G^2. \quad (17b)$$

Unfortunately, these Eqs. (17a,b) are valid for stationary PEM fuel cells and were published in 1999. Instead of using these two equations, the most updated data in Ref. [17] are used in our study, in which C_{BOP} is estimated to be 34% of fuel cell system cost, as C_{st}, including assembly, is assumed to be contributing approximately 66% of fuel cell system cost. Even though the breakdown of the fuel cell system is for an 80-kW direct hydrogen system, the same breakdown is possible to use for a 50-kW fuel cell system because the cost analysis is only integrated in the stack and BOP costs.

So, in order to build the cost model sharing the same optimization parameters, the cost model is likely to be a function of the efficiency, as in Eq. (21), which is able to investigate the impact of the cell voltage, V_c, and current density, i, as well as other optimization parameters on the fuel cell cost. In our study, the costs of the fuel cell stack and BOP are considered, and the maximum fuel cells system cost is obtained as the maximum efficiency is achieved. Thus, this cost optimization model can share the same optimization parameters with the system efficiency optimization model, and each feasible range of the parameters will be used as a constraint of this optimization problem. The base production volume is chosen as 18,000 units, which can be a mass production for the mobile 50-kW PEM fuel cell system.

$$\min C_{FC}(P_{sys}, \lambda_{H_2}, \lambda_{air}, V_c, i) = (C_{st} + C_{BOP}) \times \eta_{fc}$$

s.t.

$$\begin{aligned} &P_{sys} \geq 0.12\,\text{MPa} \\ &\lambda_{H_2} \geq 1 \\ &\lambda_{air} \geq 1 \\ &V_c \geq 0\ V \\ &i \geq 0\,\text{mA cm}^{-2} \end{aligned} \quad . \quad (21)$$

As explained in Section 2, the design variables of the cost model could be reduced to the cell current density.

In the following section, the multi-objective optimization will be presented with consideration of both efficiency and cost optimization.

4. Multi-objective optimization for PEMFC

According to the above considerations, the multi-objective optimization problem is formulated as follows:

$$\min \eta_{fc}(P_{sys}, \lambda_{H_2}, \lambda_{air}, i) = (-1)\frac{V_c u_f(P_{stack} - P_{prs})}{1.25P_{stack}}$$

$$\min C_{FC}(P_{sys}, \lambda_{H_2}, \lambda_{air}, i) = (C_{st} + C_{BOP}) \times \eta_{fc}$$

s.t.

$$\begin{aligned} &P_{sys} \geq 0.12\,\text{MPa} \\ &\lambda_{H_2} \geq 1 \\ &\lambda_{air} \geq 1 \\ &i \geq 0\,\text{mA cm}^{-2} \end{aligned} \quad . \quad (21)$$

In the multi-objective optimization problem, both objective functions have to be minimized simultaneously. The objectives in such a problem are often in conflict with each other. From Eq. (21), when the efficiency is increased, the cost increases as well. Thus, during the optimization process for such a problem, there is no single optimum solution to improve all of the objectives, which means that a number of solutions that are all optimal can exist. As the solution to the multi-objective problem is a set of points that represent the best trade-offs between the objective functions for each solution, there is no way to further improve an objective function without worsening at least one other one. Such points are called Pareto-optimal points or non-inferior points. The set of all the Pareto-optimal points is called the Pareto-optimal set or the Pareto frontier. Here, the MATLAB optimization toolbox [16] for multi-objective optimization problems is used to find the Pareto frontier solution set. MATLAB has two functions to solve multi-objective problems: fminimax and fgoalattain. Even though both methods use the popular nonlinear programming algorithm, a sequential quadratic programming (SQP) fminimax method is more appropriate for our optimization than the fgoalattain method because the latter method is more complicated than the fminimax due to the weighting coefficients. The general form of fminimax method is:

$$\min_x \max_f \{f_1, f_2, \ldots, f_m\}$$

such that

$$\begin{aligned} &Ax \leq b \\ &A_{eq}x = b_{eq} \\ &C(x) \leq 0 \\ &C_{eq}(x) = 0 \\ &L_b \leq x \leq U_b \end{aligned} \quad , \quad (22)$$

where x is the design variable vector, $f_1, f_2, \ldots, f_m$ are the objective functions, matrix A and vector b are the coefficients of the linear inequality constraints, matrix A_{eq} and vector b_{eq} are the coefficients of the linear equality constraints, C contains the nonlinear inequality constraints, C_{eq} contains the nonlinear equality constraints, and L_b and U_b are the lower and upper bounds, respectively. In order to search for the optimal design value x, the fminimax method iteratively minimizes the worst-case value (or maximum) of the objective functions subject to the constraints. The advantage of this method is to easily find the optimum design from an arbitrary initial design point. Furthermore, less function and gradient evaluation are required compared with other constrained nonlinear optimization methods. However, the main

disadvantages of both methods, fminimax and fgoalattain, are that the objective functions must be continuous and that each method has a limitation in searching for global solutions.

5. Results and discussion

In this section, the fminimax method is executed to solve the multi-objective optimization. To avoid the unrealistic design criterion, the upper bounds of the system pressure and the air and hydrogen stoichiometric ratios are specified at 10, 10 and 10 MPa, respectively. According to the polarization *I–V* curve in Fig. 1, the cell current density will lie within the range of 0–1 A cm^{-2}, which is used as one of bound limits for the optimization. The bound limits of the design variables are given as follows:

$$\begin{aligned} &0.12\,\text{MPa} \le P_{\text{sys}} \le 10\,\text{MPa} \\ &1 \le \lambda_{H_2} \le 10 \\ &1 \le \lambda_{\text{air}} \le 10 \\ &0 \le i \le 1\,\text{A cm}^{-2} \end{aligned} \quad . \tag{23}$$

With various initial conditions of the design parameters, P_{sys}, λ_{H_2}, λ_{air}, and i, corresponding trade-offs (Pareto) solutions are obtained. So to speak, these solutions are in the Pareto set; that is, as one objective is improved in the set the other is worsened.

For simplicity, the initial conditions can be described in the column vector, such as [P_{sys}, λ_{H_2}, λ_{air}, i]. If an arbitrary initial condition is defined as the vector, In 1 = [0.12 MPa, 2, 2, 800 mA cm^{-2}], Fig. 3 shows the trade-off solution based on the vector In 1. In Fig. 3, as the efficiency is improved in the set, the cost is increased as well. In changing the initial condition, this Pareto frontier will be changed because the fminimax method will find a local solution in the changed initial condition. First, when In 1 is changed to ln 2 = [0.24 MPa, 2, 2, 800 mA cm^{-2}] – that is, the system pressure becomes two times larger than the one for In 1 – Fig. 4 shows how this change affects the optimization of the fuel cell. As seen in Fig. 4, the higher system pressure is able to achieve a cost-effective and high-performance model compared with the model given by ln 1. For instance,

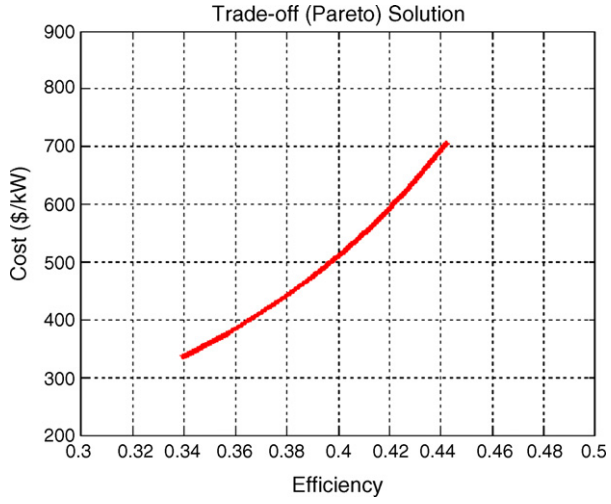

Fig. 3. Pareto frontier based on the ln 1. ln 1 = [0.12 MPa, 2, 2, 800 mA cm^{-2}].

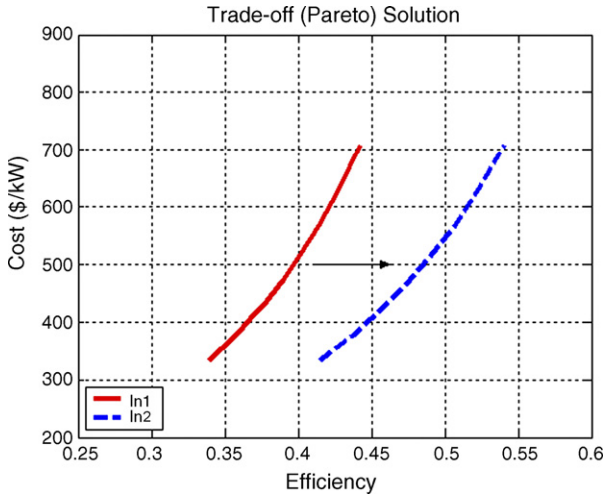

Fig. 4. Pareto frontier change from ln 1 to ln 2. ln 2 = [0.24 MPa, 2, 2, 800 mA cm^{-2}].

in Fig. 4, at the efficiency 0.45, the ln 2 Pareto frontier corresponds to about 420 US$ kW^{-1}, whereas in ln 1 the Pareto frontier is almost 700 US$ kW^{-1} than mean In 1 is less economic condition than the ln 2. However, in the case of much higher pressure, the change from ln 1 to ln 3 = [0.36 MPa, 2, 2, 800 mA cm^{-2}], as shown in Fig. 5, although a better optimum model than In 2 is obtained, the efficiency range of ln 3 becomes unrealistic because the fuel cell system efficiency is not normally greater than 0.6 [1]. Hence, the initial condition ln 2 is more recommendable than ln 3. Second, if the initial hydrogen stoichiomertic ratio is changed from 2 to 1.5, such as ln 4 = [0.12 MPa, 1.5, 1, 800 mA cm^{-2}], the less cost-effective and poorer performance model is found in Fig. 6. Hence, around the hydrogenstoichiomertic ratio, 2 is more preferable than 1.5.

In the case that the air stoichiometric ratio is changed from 2 to 1.5 as the In 5 = [0.12 MPa, 1.5, 1, 800 mA cm^{-2}], the more cost- and efficiency-effective model is achieved in Fig. 7. However, if it keeps decreasing to 1, the efficiency is not applicable to the real system as seen in Fig. 8. Hence, the ratio around 1.5 is more preferable than 2 and 1. For the current density, as it decreases, the cost- and efficiency-effective model is achieved.

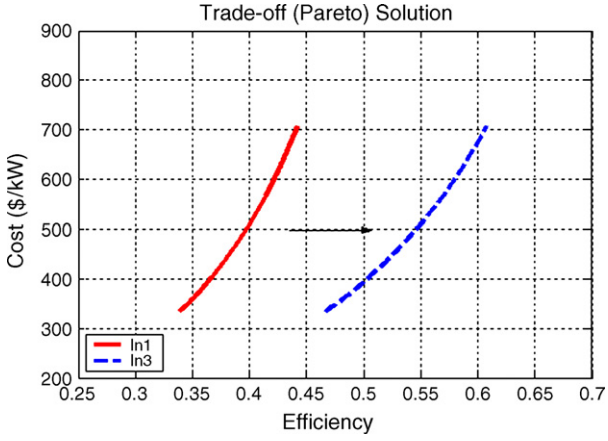

Fig. 5. Pareto frontier change from In 1 to In 3. In 3 = [0.36 MPa, 2, 2, 800 mA/cm^2].

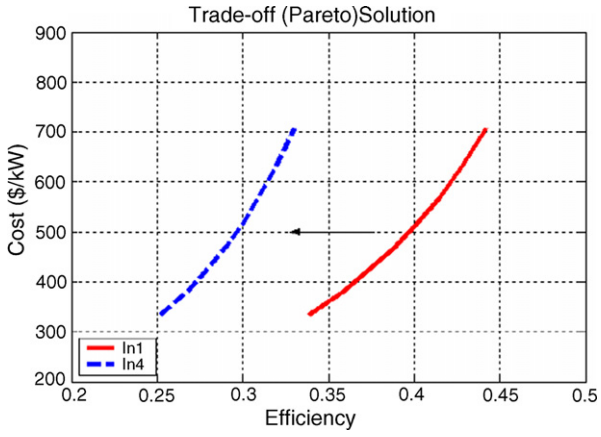

Fig. 6. Pareto frontier change from In 1 to In 4. In 4 = [0.12 MPa, 1.5, 2, 800 mA cm^{-2}].

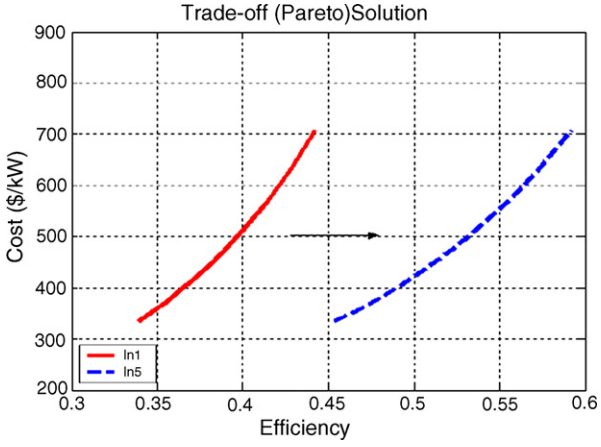

Fig. 7. Pareto frontier change from In 1 to In 5. In 5 = [0.12 MPa, 2, 1.5, 800 mA cm^{-2}].

Through trial and error, the optimal current density is approximately estimated to be 450 mA cm^{-2}. Comparing this with In 1, In 7 provides a better performance- and cost-effective model, as shown in Fig. 9. With the recommended current density of 450 mA cm^{-2} and the *V–I* polarization curve shown in Fig. 1,

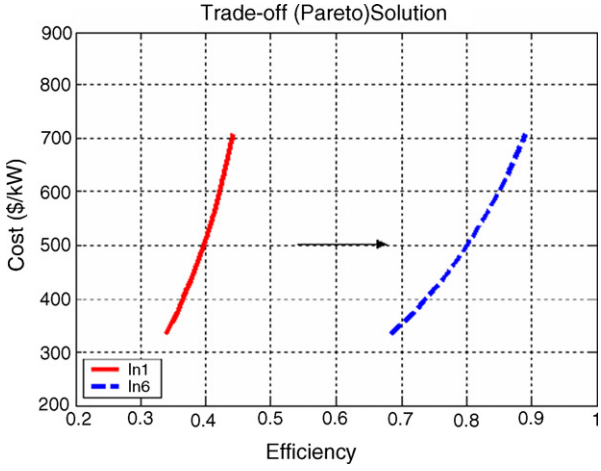

Fig. 8. Pareto frontier change from In 1 to In 6. In 6 = [0.12 MPa, 2, 1, 800 mA cm^{-2}].

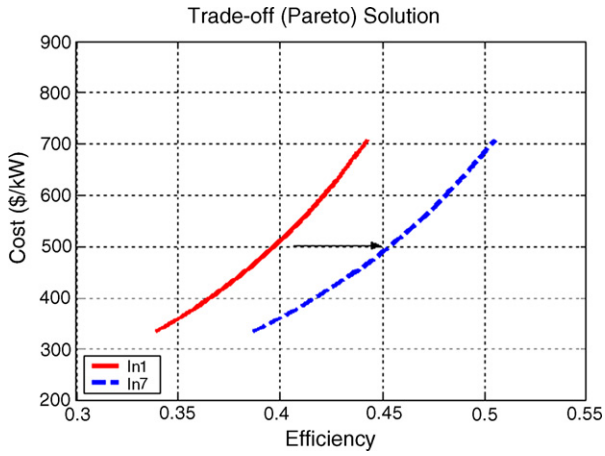

Fig. 9. Pareto frontier change from In 1 to In 7. In 7 = [0.12 MPa, 2, 2, 450 mA cm^{-2}].

the optimal cell voltage can be calculated to be 0.72 V, and the power density will be 3.2 kW m^{-2}. If a 50-kW rate power output is selected, then the total active cell area is 15.625 m^2, which means the stack will need to contain 174 layers of a single cell with 30 cm × 30 cm active cell area. Thus, the optimal current density allows us to determine the total active cell area and even to provide the information about the cell number required for the target stack if the a single cell area is given.

Figs. 4–11 indicates that the change of each design variable has a severe impact on the cost and efficiency of the fuel cell. Because the current density, in particular, is closely associated with the fuel cell area, it has a more direct effect on the fuel cell cost and efficiency than any of the other variables.

When selecting the preferable initial condition, In 8 = [0.24 MPa, 2, 1.5, 450 mA cm^{-2}], based on the above discussion, the Pareto solution is achieved in Fig. 10, but it is definitely not applicable to the real system due to an impractically high efficiency. Therefore, In 8 must be adjusted such that the Parteto solution lies in a realistic range. As In 8 = [0.24 MPa, 2, 1.5, 450 mA cm^{-2}] is adjusted to In 9 = [0.24 MPa, 1.75, 1.5, 450 mA cm^{-2}], this condition can be used for the design

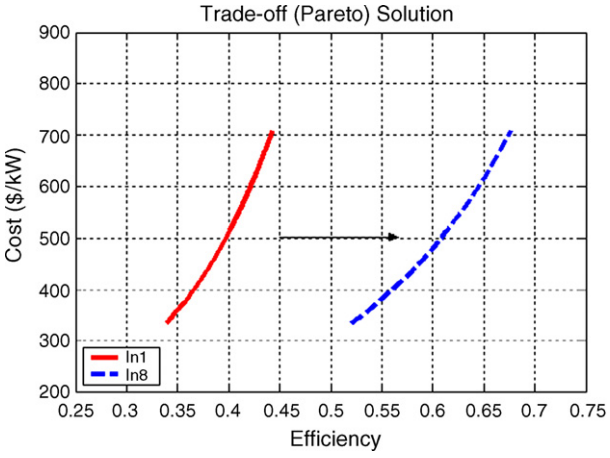

Fig. 10. Pareto frontier change from In 1 to In 8. In 8 = [0.24 MPa, 2, 1.5, 450 mA cm^{-2}].

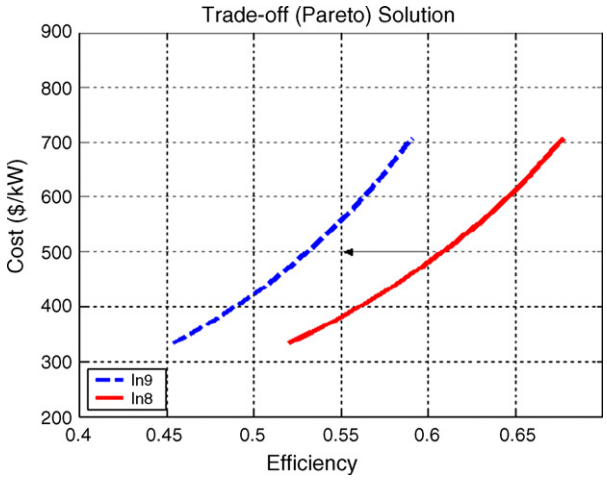

Fig. 11. Pareto frontier change from In 8 to In 9. In 9 = [0.24 MPa, 1.75, 1.5, 450 mA cm^{-2}].

of an economic and high-performance fuel cell. Any initial condition can be chosen as long as it is within the bound limits and the corresponding Pareto solutions are applicable in practice.

6. Conclusion

In the paper, a joint optimization model of fuel cell system efficiency and cost is proposed. A multi-objective optimization technique, the sequential quadratic programming method, has been applied to investigate the impact of the variations of initial conditions on the efficiency and cost of a fuel cell system. Although the study shows that the change of current density is more closely related to the fuel cell efficiency and cost than to any other variables, the system pressure, the hydrogen and air stoichiometric ratios, and the current density must be appropriately selected for the optimal design because they also largely affect the fuel cell system and cost, as well, in the our study. Our work presents a way to determine the optimal design regarding the fuel cell efficiency and cost aspects simultaneously.

References

[1] J. Larminie, A. Dicks, Fuel Cell Systems Explained, Wiley, New York, 2002.
[2] Y.J. Zhang, M.G. Ouyabg, Q.C. Lu, J.X. Luo, X.H. Li, Appl. Therm. Eng. 24 (4) (2004) 501–513.
[3] F. Barbir, T. Gomez, Int. J. Hydrogen Energy 22 (10/11) (1997) 1027–1037.
[4] D. Xue, Z. Dong, J. Power Sources 76 (1998) 69–80.
[5] C.C. Boyer, R.G. Anthony, A.J. Appleby, J. Appl. Electrochem. 30 (2000) 777–786.
[6] S.E. Isuke, A.B. Mohamad, A.A. Kadhum, W.R.W. Daud, C. Rachid, J. Power Sources 114 (2003) 195–202.
[7] C.A. Frangopoulos, L.G. Nakos, Energy 31 (2006) 1501–1519.
[8] U.S. Department of Energy, Fuel cell handbook, sixth ed., EG&G Technical Service Inc., 2002.
[9] B. Blunier, A. Miraoui, Vehicle Power and Propulsion 2005 IEEE Conference, 2005.
[10] P. Pei, W. Yang, P. Li, Int. J. Hydrogen Energy 31 (2006) 361–369.
[11] J.M. Cunningham, M. Hoffman, et al., Proceedings of the 17th International Electric Vehicle Symposium and Exposition, Montreal, Canada, October, 2000.
[12] F. Barbir, PEM Fuel Cells Theory and Practice, Elsevier Inc., 2005.
[13] C.E. Tomas, J.P. Barbour, B.D. James, F.D. Lomax, Cost Analysis of Stationary Fuel Cell Systems Including Hydrogen Cogeneration, National Renewable Energy Laboratory, Colorado, 1999 (ACG-8-18012-02).
[14] F. Laurencelle, R. Chahine, J. Hamelin, K. Agbossou, M. Frournier, T.K. Bose, A. Laperrriere, Fuel Cells (1) (2001) 66–71.
[16] E.J. Carlson, P. Kopf, Sinha, S. Sriramulu, Y. Yang, TIAX LLC, Cambridge, MA, 2005.
[17] H. Tsuchiya, O. Kobayashi, Int. J. Hydrogen Energy 29 (2004) 985–990.
[18] S. Kamarudin, W. Daud, A. Som, M. Takriff, A. Mohammad, J. Power Sources 157 (2006) 641–649.